Propagation Behavior of Root Crack in Weld Metal of High Strength Steel on the Basis of AE Source Location Technique †
– Application of Acoustic Emission Technique for Weld Cracking (III) –

Fukuhisa MATSUDA*, Hiroji NAKAGAWA**, Yoshinori MORIMOTO*** and Hiroshi KIHARA****

Abstract

AE source location technique is applied to restraint cracking test of HY-type HT90 high strength steel with Y-groove where the root crack has a tendency to initiate and propagate in the weld metal. It is shown that AE events have a tendency to concentrate in places where the root cracks are propagating toward the surface of weld metal. This behavior is caused by anisotropy of propagation of hydrogen-induced crack in weld metal, and is quite different from that in the case where the root crack initiates and propagates in the heat-affected zone.

KEY WORDS: (Acoustic Emission) (High Strength) (Cold Cracking) (Restraint) (Hydrogen Embrittlement)

1. Introduction

In a previous paper[1] the authors studied the behavior of root crack which propagated through the heat-affected zone except for the final stage just before the complete cracking, using AE source location technique for restraint cracking test. According to the results, root cracks occurred at several sites of the root edge have a tendency to unite easily with one another by their propagation along the welding direction instead of their propagation toward the surface of weld metal.

On the other hand, the root crack occurred in the TRC test of HY110 and HY130 initiates easily in the weld metal and propagates as a fan-like pattern from a part at the root edge[2]. This is perhaps due to anisotropy of propagation behavior of hydrogen-induced crack in the weld metal. Consequently, it is supposed that the propagation behavior of the root crack and thus the behavior of AE in these steels are quite different from those in the previous paper[1].

Therefore, in this study AE source location technique was applied to restraint cracking test of HY-type HT90, and the propagation behavior of root crack and the behavior of AE were discussed.

2. Materials Used and Experimental Procedures

A weldable heat-treated high strength steel HT90 corresponding to HY110 whose yield strength was about 80kg/mm^2 was used for restraint cracking test. The chemical composition is 4Ni-Cr-Mo-V type. The configuration of test specimen is shown in **Fig. 1**, in which a

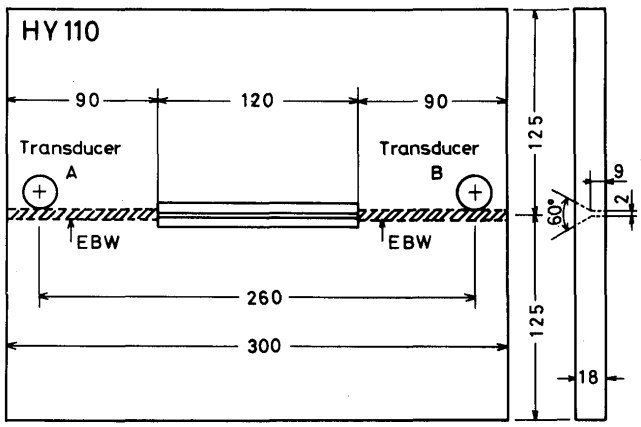

Fig. 1 Specimen configuration of restraint cracking test with Y-groove

Y-groove was machined in order that the root crack passed mainly the weld metal. The restraint welding in both sides of the groove was done with electron beam welding by each one pass from top and back surfaces.

† Received on March 31, 1979
* Professor
** Research Instructor
*** Former Graduate Student of Osaka Univ., now with Komai Iron Works Co., LTD.
**** Emeritus Professor of Tokyo and Osaka Univ.

The restraint intensity in the middle of groove length was about 1200kg/mm·mm according to the formula in case of uniformly distributed loads which was derived by Ueda, et al[3].

Shielded metal-arc welding was done with a tentative electrode of low hydrogen type whose deposited metal had a tensile strength of about 100kg/mm^2. The chemical composition of the deposited metal is 2.5Ni-Cr-Mo type. Baking condition of the electrode and preheating temperature of the test specimen were varied in order to obtain various crack sizes. The welding conditions were 170A, 25V and 150mm/min, and the starting part and the crater of the weld bead were turned away from the root gap in order to avoid the occurrence of weld defects. Immediately after the welding, slags on the bead surface were completely removed.

Then, two AE transducers were set on the test specimen as shown in Fig. 1, and AE measurement was started from 2min after the completion of welding. The monitoring system, the procedure and the conditions of AE measurement were just the same as those in the previous paper[1]. The AE parameters measured were AE cumulative count, AE cumulative event count, AE source location, maximum ringdown counts per event and S value[1].

The AE measurement was stopped after the testing of 48hr and the test specimen was immediately taken into an electric furnace of about 350°C in order to oxidize the crack surface. Subsequently the test specimen was fractured with a bending test machine at room temperature. However, as regards fully cracked specimen, the oxidizing treatment was omitted. Then, the distribution and the size of cracks were measured with a planimeter on the light fractograph.

Table Summary of the results of restraint cracking test and AE measurements

Specimen number	Baking condition of electrode (°C x hr)	Preheating temperature (°C)	Cracked area (mm^2)	Crack ratio* (%)				AE data			
				C_a	C_s	C_f	C_r	Cumulative count**	Cumulative event count	S value	Max. ringdown counts/event
1	400 x 1	80	1	0.2	0	0	4	58	3	>3	< 100
2	400 x 1	85	1	0.2	0	0	5	3300	26	2.1	1000
3	400 x 1	85	3	0.4	2	0	8	1500	7	1.05	1100
4	390 x 1	70	4	0.7	0	0	11	7200	34	1.58	1600
5	400 x 1	75	212	33	23	0	44	29200	45	0.4	8200
6	380 x 1	room temp.	610	100	100	100	100	568900	331	0.45	>10000
7	240 x 1	room temp.	617	100	100	100	100	351900	304	0.51	>10000

* C_a is crack ratio on fractured surface, C_s is cross sectional crack ratio, C_f is surface crack ratio and C_r is root crack ratio.
** AE cumulative count is the mean value of two channels.

3. Experimental Results and Discussions

Table 1 shows summary of the results of the restraint cracking test and the AE data, where C_a, C_s, C_f and C_r are crack ratios defined in the previous paper[1]. Namely, C_a is crack ratio on fractured surface, C_s is cross sectional crack ratio, C_f is surface crack ratio and C_r is root crack ratio. Lowering the baking condition of electrode and the preheating temperature of test specimen increased the crack ratios.

3.1 Case I: Completely Cracked Specimen

Figure 2 shows the changes in AE cumulative count and AE cumulative event count vs. time in specimen No.7, and **Fig. 3** shows the change in AE source location in the same specimen during the time intervals shown in Fig. 3. Relative location in the abscissa in Fig. 3 is defined to be 0% at the left transducer and 100% at the right one in Fig. 1, and the increase in the relative location agrees with the welding direction. Considering the error in AE source location in the AE monitoring system[4], the AE emitted in the weld metal must lie between about 20 and 80% of

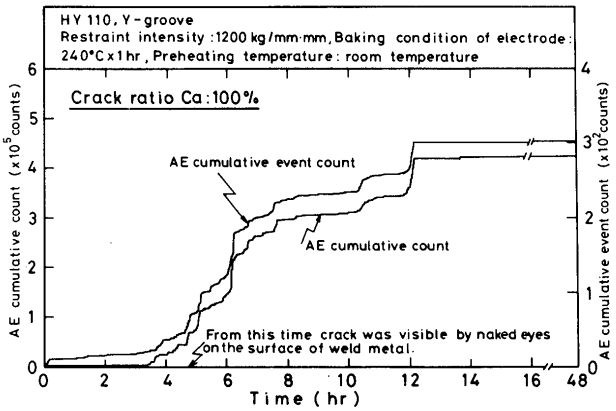

Fig. 2 Changes in AE cumulative count and cumulative event count vs. time in specimen No. 7

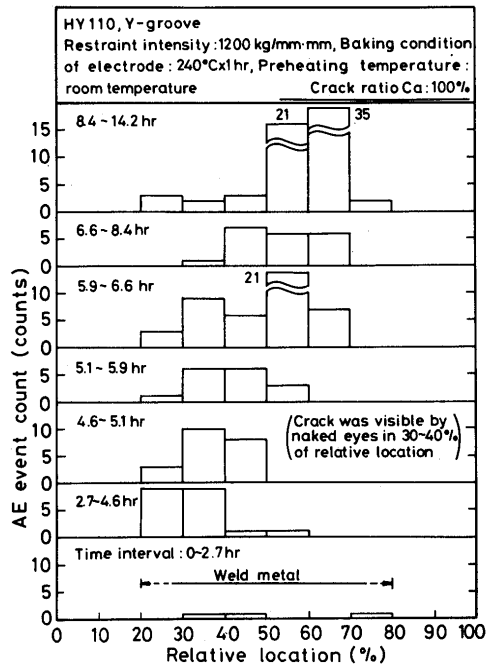

Fig. 3 Change in AE source location vs. time in the same specimen as that in Fig. 2

relative location, the range of which is indicated by arrows in Fig. 3.

In Fig. 2 both AE cumulative count and event count were very little till about 2.7hr, when AE events were sporadic along the weld length in Fig. 3. Then, in Fig. 2 both AE cumulative count and event count increased gradually from about 2.7 to 4.6hr, when AE events concentrated in 20 to 40% of relative location. Subsequently at about 4.6hr, crack was visible with the naked eyes on the surface of weld metal in 30 to 40% of relative location, when AE events also concentrated in and around 30 to 40% in Fig. 3. Furthermore, in Fig. 2 AE cumulative count and event count continued to increase till about 12hr, when the crack on the surface of weld metal propagated gradually toward the crater according to the observation with the naked eyes. During this period, the relative location where AE events concentrated shifted toward the larger value, namely the crater side, which agrees well with the observation with the naked eyes. Finally at about 12hr, the specimen cracked almost completely, and thus the AE cumulative count and event count increased very slightly after about 12hr.

Therefore according to the results of AE source location, the propagation behavior of this root crack is as follows: A crack in the first place occurred at the root edge near the starting part of weld bead, then propagated toward the surface of weld metal. Subsequently other different cracks occurring one after another at parts of the root edge in the crater side propagated toward the surface of weld metal, and then the final fracture occurred near the crater.

The final AE source location is shown in **Fig. 4.** It is

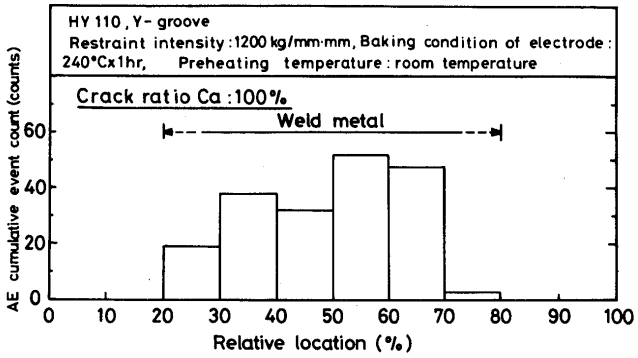

Fig. 4 Final AE source location in the same specimen as that in Figs. 2 and 3

noted that there are more AE events in 50 to 70% of relative location, where the crack was lastly observed on the surface of weld metal.

These behaviors of AE source location are quite different from those in the previous paper[1]. Moreover it is noticed that the average increasing rates of AE cumulative count and event count after the first emergence of crack on the surface of weld metal are gentle compared with those in the previous paper[1]. Besides, in final AE source location there are more AE events in the place where the crack was lastly observed on the surface of weld metal, but in the place where the crack was first observed in the previous paper[1]. It is considered that these are due to the difference of propagation behavior of root crack.

The macrofractograph of this specimen and its sketch, which is written with a magnification of about two times in only the height direction, are shown in **Fig. 5.**

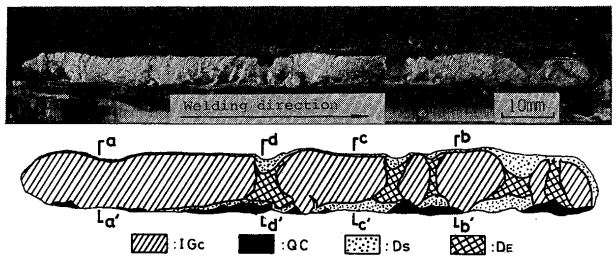

Fig. 5 Light fractograph and its sketch of the same specimen as that in Figs. 2 to 4

Moreover for the sake of good understanding of the behavior of the crack propagation, the transverse cross sections along a-a', b-b', c-c' and d-d' in Fig. 5 are shown in **Figs. 6(a), (b), (c) and (d)** respectively. The cracked

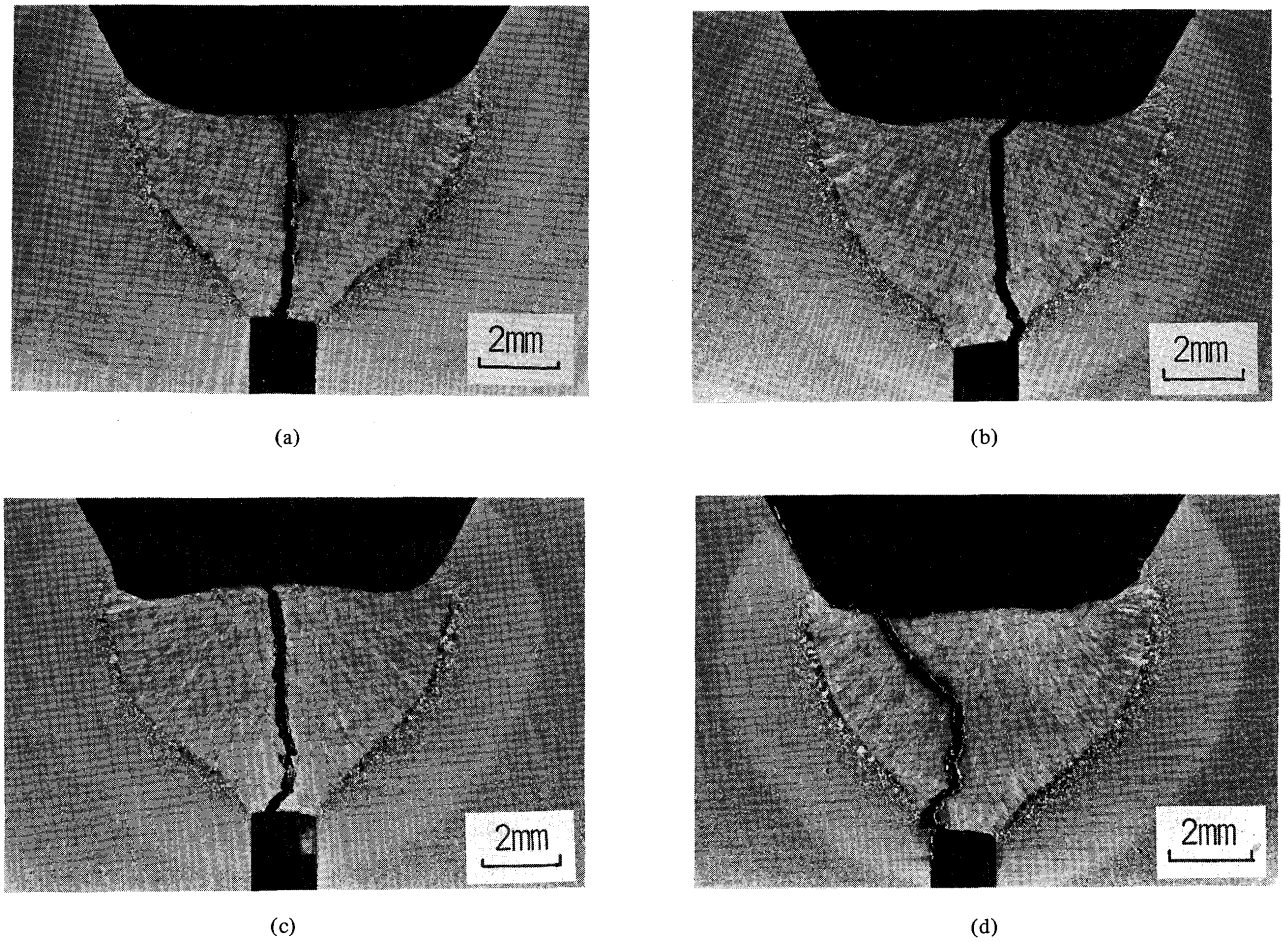

Fig. 6 Macrostructures of transverse cross sections along (a) a-a , (b) b-b′, (c) c-c′ and (d) d-d′ in Fig. 5

surface in Fig. 5 is composed of IG_c, QC, D_E and D_s regions. The IG_c region macroscopically gives a directional and brilliant appearance, and microscopically gives a feature shown in **Fig. 7(a)** which is mainly composed of intergranular fracture along columnar crystal boundary of prior austenite (IG_c) and partly of quasi-cleavage affected by hydrogen. The IG_c region cracked in the weld metal. The QC region macroscopically gives a non-directional and

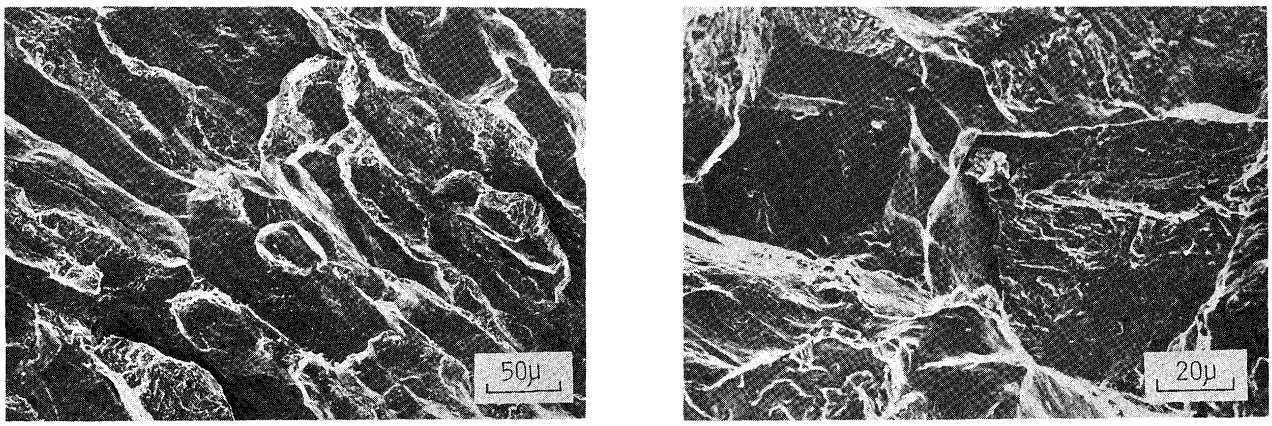

(a) mainly intergranular and partly hydrogen-induced quasi-cleavage fractures in weld metal (defined as IG_c region)

(b) mainly hydrogen-induced quasi-cleavage and partly intergranular fractures in heat-affected zone (defined as QC region)

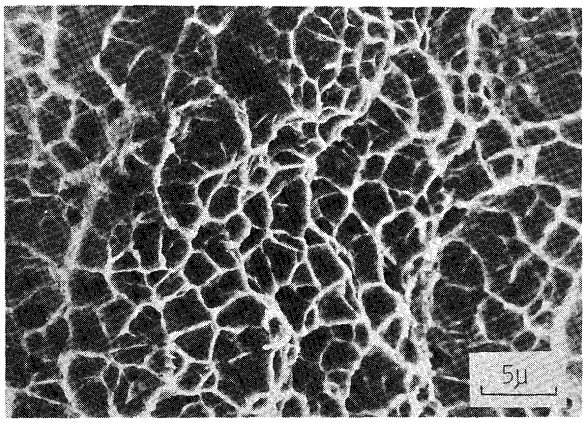

(c) Equiaxed dimple fracture (defined as D_E region)

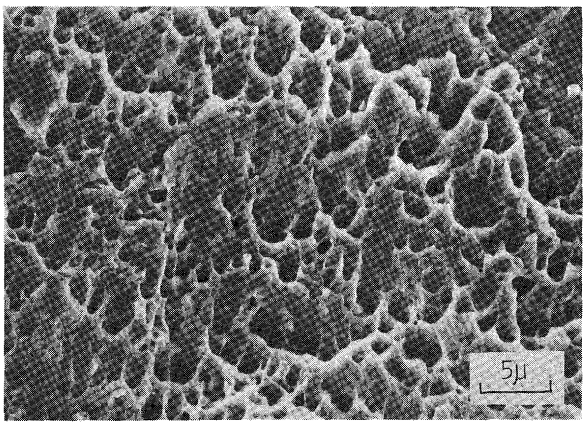

(d) Shear dimple fracture (defined as D_S region)

Fig. 7 Typical microfractographs of root crack in Fig. 5 with a scanning electron microscope

brilliant appearance, and microscopically gives a feature shown in **Fig. 7(b)** which is mainly composed of quasi-cleavage (QC) affected by hydrogen and partly of non-directional intergranular fracture. The QC region cracked in the heat-affected zone. The D_E region is macroscopically dull and silky gray in appearance, and microscopically gives equiaxed dimple fracture (D_E) shown in **Fig. 7(c)**. The D_s region is also macroscopically dull, silky gray in appearance, and microscopically gives shear dimple fracture (D_S) shown in **Fig. 7(d)**.

In Fig. 5, D_E region is seen in only the crater-side's half portion, and there is far more D_S region in this portion than in the other portion. These well support the propagation process estimated by AE source location in Fig. 3.

3.2 Case II: Partly Cracked Specimen

Figure 8 shows the changes in AE cumulative count and event count vs. time in specimen No.5 whose crack ratio on fractured surface was 33%, and **Fig. 9** shows the

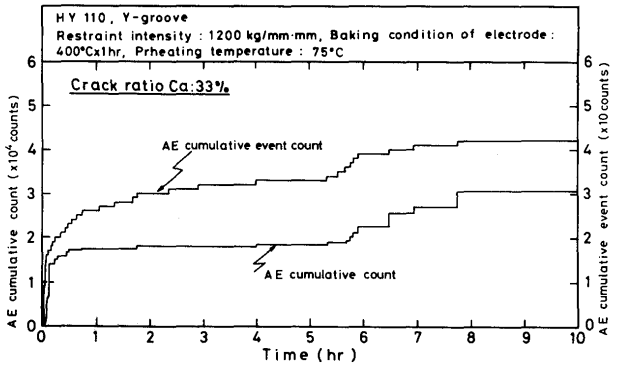

Fig. 8 Changes in AE cumulative count and cumulative event count vs. time in specimen No.5

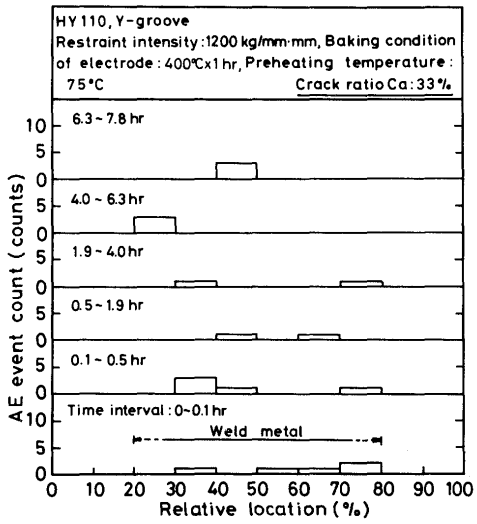

Fig. 9 Change in AE source location vs. time in the same specimen as that in Fig. 8

change in AE source location. In Fig. 8, both AE cumulative count and event count increased gradually and intermittently till about 7.8hr, and they stopped. In Fig. 9 AE events seem to be sporadic or somewhat scattered along the weld length during this period*, nevertheless it is recognized that AE events have a tendency to concen - trate in about 30% and 40 to 50% of relative location. The final AE source location is shown in **Fig. 10.**

The macrofractograph of this specimen and its sketch are shown in **Fig. 11**, where A_F is artificially fractured region after the cracking test. Developed two IG_c regions are seen near the starting part and the middle part of the weld bead, and these agree with the behavior of AE events in Fig. 9. In Fig. 11, however, several tiny QC regions at the root edge are scattered along the weld bead. The AE events which are considered to be due to them are

* The authors consider that slags at the root edge might give rise to some AE in the early stage and that this causes somewhat scattered impression in Fig. 9, because the increasing rate during 0 to 0.1hr in Fig. 8 is somewhat abnormal as compared with that in Fig. 2 taking care of difference in scale between these figures. In Fig. 2 an incubation period is rather clearly seen in spite of the fully cracked specimen.

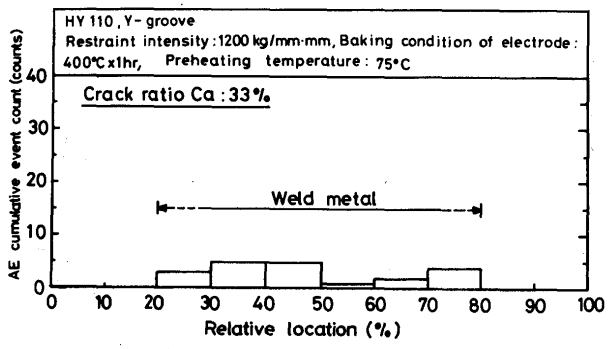

Fig. 10 Final AE source location in the same specimen as that in Fig. 8 and 9

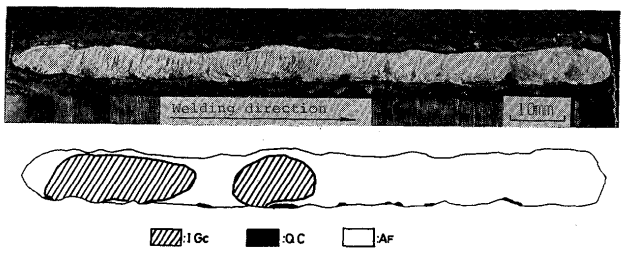

Fig. 11 Light fractograph of artificially fractured surface containing root crack and its sketch of the same specimen as that in Figs. 8 to 10. A_F: artificially fractured region after cracking test

observed in Fig. 9, and it is understood from Fig. 9 that their propagation stopped by 4hr.

Figure 12 shows the changes in AE cumulative count and event count vs. time in specimen No.1 whose crack ratio on fractured surface was 0.2%. In Fig. 12 the AE stopped at about 1.7hr. The final AE source location shown in **Fig. 13** agrees well with the macrofractograph and its sketch in **Fig. 14** where only a few tiny cracks are seen at the somewhat left from the middle part of weld length.

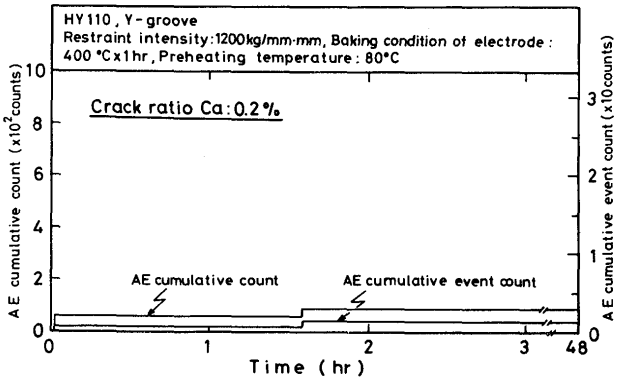

Fig. 12 Changes in AE cumulative count and cumulative event count vs. time in specimen No.1

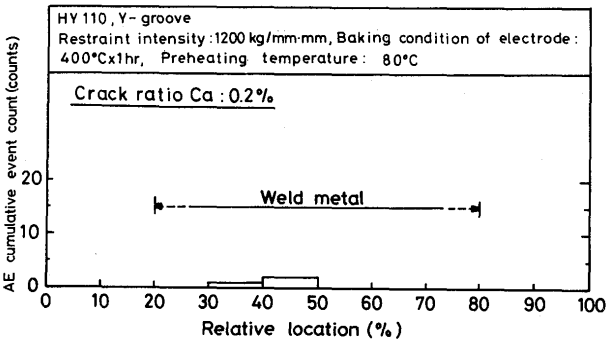

Fig. 13 Final AE source location in the same specimen as that in Fig. 12

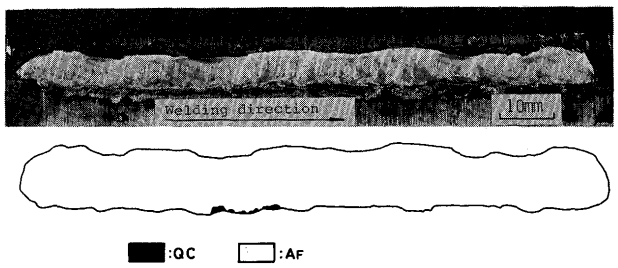

Fig. 14 Light fractograph of artificially fractured surface containing root crack and its sketch of the same specimen as that in Figs. 12 and 13

3.3 Estimation of Propagation Behavior of Root Cracking

The behaviors of AE mentioned above are quite different from those in the previous paper[1] where AE emitted together with the root crack propagating through heat-affected zone were discussed. In the previous paper[1], the AE didn't concentrate somewhere but scattered from place to place all over the whole length of weld bead, and this was correlated to the fact that root cracks occurring at several sites of the root edge have a tendency to unite easily with one another by their propagation along the welding direction instead of their propagation toward the surface of weld metal. On the other hand, in this study, the AE events have a tendency to concentrate somewhere in the weld length as seen in Fig. 3. Judging from the cracked surface shown in Figs. 5 and 11, it is recognized that this tendency of AE events was caused by anisotropy of propagation behavior of hydrogen-induced crack along columnar crystal boundary in the weld metal.

Considering the results in Figs. 2 to 14 and other data together, the propagation behavior of root crack in this study is estimated as in **Fig. 15**. The root cracks in the first place occur in the weld metal at a few sites of root edge (Stage 1). They propagate mainly toward the surface of weld metal by the anisotropy effect, and at the same time tiny root cracks occur partly in the heat-affected zone (Stage 2). Then they propagate further and a part of

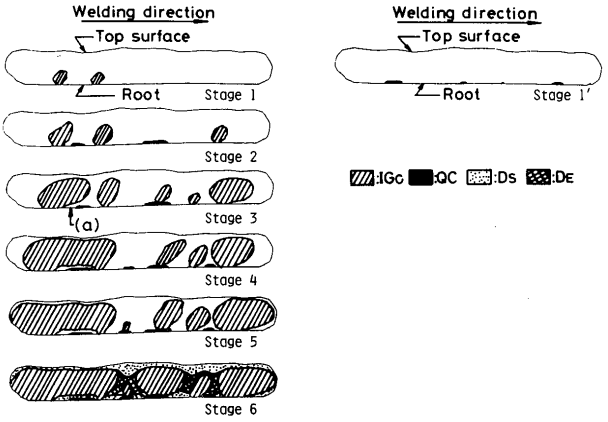

Fig. 15 Estimated propagation behavior of root crack

them reaches the surface of weld metal, and root cracks in the heat-affected zone easily turn into the weld metal (Stage 3). Subsequently, the adjacent root cracks in weld metal unite each other to propagate (Stages 4 and 5). Finally, when the stress condition of the portion which has remained uncracked becomes a critical condition, this portion fractures rapidly (Stage 6). If the diffusible hydrogen content is relatively low, the root cracks stop sometime between Stages 1 and 5. If the diffusible hydrogen content is extremely low, only tiny root cracks occur in the heat-affected zone (Stage 1').

4. Conclusions

Main conclusions obtained are as follows; The root crack in restraint cracking test of HY110 has a tendency to initiate and propagate in the weld metal. Moreover, the crack has a tendency to grow toward the surface of weld metal because of anisotropy of propagation behavior of hydrogen-induced crack in weld metal. Therefore AE events also have a tendency to concentrate in places where the cracks are propagating toward the surface of weld metal. This behavior of AE is quite different from that in the case where the root crack initiates and propagates in the heat-affected zone discussed in the previous paper.

References

1) F. Matsuda, et al: Trans. JWRI, Vol.7 (1978), No.2, pp.203-214.
2) F. Matsuda, et al: Trans. JWRI, Vol.6 (1977), No.2, pp.219-233.
3) Y. Ueda, et al: Trans. JWRI, Vol.7 (1978), No.1, pp.11-16.
4) F. Matsuda, et al: Trans. JWRI, Vol.7 (1978), No.1, pp.87-92.